J Mater Sci (2007) 42:4308–4315
DOI 10.1007/s10853-006-0653-z

Influence of pad span on fretting fatigue behaviour of AISI 304 stainless steel

M. Jayaprakash · S. Ganesh Sundara Raman

Received: 7 December 2005 / Accepted: 7 July 2006 / Published online: 28 February 2007

Abstract The present work deals with the influence of pad span on fretting fatigue behaviour of AISI 304 stainless steel. Relative slip is one of the three primary variables influencing fretting fatigue behaviour. The relative slip can be modified by changing the pad span and/or cyclic stress. In the present study, the effect of relative slip was studied at different cyclic stress levels and by using fretting pads with three different pad span values (15, 20 and 30 mm). The relative slip increased with an increase in pad span and cyclic stress. Samples tested with fretting pads having longer pad span (30 mm) exhibited longer lives. Though the specimens tested with pads having longer pad span experienced higher frictional stress and tangential force coefficient compared with those tested with pads having smaller pad span (15 or 20 mm), the relative slip values were larger in the former. Due to larger relative slip values it was assumed that small cracks initiated by fretting fatigue would have been worn away due to wear damage. Due to this the specimens tested with pads having longer pad span exhibited enhanced fretting fatigue lives. More deformation-induced martensite formed in the samples tested with pads having longer pad span owing to longer lives.

M. Jayaprakash · S. Ganesh Sundara Raman (✉)
Department of Metallurgical and Materials Engineering, Indian Institute of Technology Madras, Chennai 600036, India
e-mail: ganesh@iitm.ac.in

Introduction

Fretting fatigue is a serious problem in engineering applications, where two components are in contact and one of them is subjected to cyclic loading. Fretting, a small amplitude oscillatory relative motion between contacting components, creates surface and subsurface damage from which fatigue cracks nucleate and grow in the presence of a cyclic load. This can occur at stress levels well below the fatigue limit of a material [1]. Practical examples of fretting fatigue failures are gas turbines, steam turbines, wheel shafts, bolted plates, wire ropes and springs.

Many factors influence fretting fatigue behaviour including contact pressure, relative slip amplitude, coefficient of friction, surface condition, microstructure, etc. [2]. Relative slip is considered as one of the primary variables influencing the effect of fretting on fatigue. The effect of relative slip on fretting fatigue life has been studied by many researchers [3–9]. Few researchers found that fretting fatigue strength (or) life decreased with an increase in amplitude of slip [4, 9]. Many researchers found that the fatigue strength (or) life showed a minimum at certain relative slip amplitude, e.g. Ref. [10]. There is a general agreement in the literature that the effect of fretting is more severe for a slip amplitude of about 20–25 μm [1].

Relative slip in fretting fatigue tests has been controlled by many techniques, e.g. normal contact load and bulk cyclic stress [5] and pad geometry [11, 12]. However, these methods do not provide the relative slip as an independent control mode. For independent control, dual actuator-based set up has been employed [7, 8, 13]. One actuator controls the fretting pad displacement and the other actuator controls the cyclic

stress on the specimen. Relative slip may be changed by changing the pad span (pad span is the distance between two pad feet) and/or cyclic stress. In the present work the effect of relative slip on fretting fatigue behaviour of AISI 304 stainless steel at different cyclic stress levels was investigated by varying the pad span.

Experimental details

The chemical composition (in wt.%) of the test material (AISI 304 stainless steel) was 0.03 C, 18.29 Cr, 8.91 Ni, 2 Mn, 1 Si and balance Fe. The material was subjected to a solution annealing treatment at 1,050 °C for 0.5 h and water quenched. The resulting grain size was 43 μm. About 6 mm thick specimens of 65 mm gauge length and 10 mm gauge width were used for fretting fatigue tests. The gauge portions of all samples were polished with four grades (1/0, 2/0, 3/0 and 4/0) of silicon carbide emery papers and cleaned with acetone. The residual polishing marks were along the length of the specimens. The room temperature mechanical properties of the material AISI 304 stainless steel were: yield strength of 220 MPa, ultimate tensile strength of 607 MPa, elongation of 68% and hardness of 210 HV_5.

An experimental facility, with a ring-type load cell and bridge-type fretting pads, which can simulate the fretting fatigue conditions, developed in-house, was used (see Fig. 1). Full details are given elsewhere [14]. Fretting pads were made of the same test material AISI 304 stainless steel. The fretting pad and loading pad were assembled as shown in Fig. 2. A proving ring was used in the fretting fatigue tests to apply the contact load. Four strain gauges were pasted on the proving ring (two on the inner surface and two on the outer surface) and wired to create a Wheatstone bridge

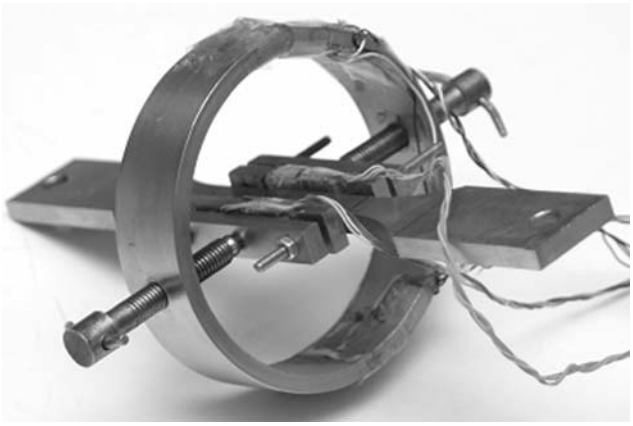

Fig. 1 Photograph of fretting fatigue test assembly

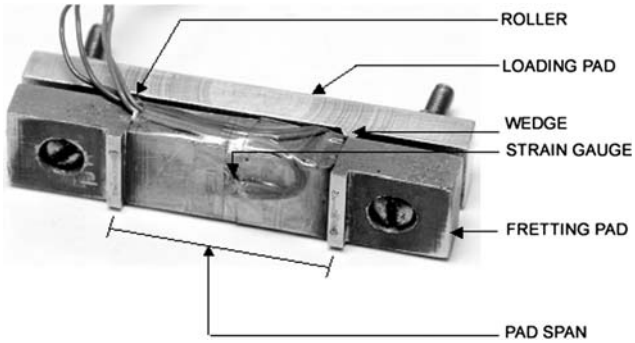

Fig. 2 Fretting pad assembly

circuit to measure the elastic strains induced by loading the ring. Frictional force between the fretting pad and the specimen was measured by bonding two strain gauges to each fretting pad (one on the inner side and the other on the outer side), with the strain gauge grid centred between the pad feet.

To measure the displacement of specimen (in the gauge portion) and pad the following method was adopted. Two steel strips were fixed—one on the top of the pad and the other on the specimen surface using an adhesive. Non-contact inductive displacement sensors (Micro-Epsilon make) were positioned above the strips in order to measure the displacement of pad and the specimen during tests. The difference between the two displacement ranges was calculated to obtain the relative slip values. A photograph of the fretting fatigue test assembly gripped in a testing machine along with the arrangement to measure displacements of specimen and pad is shown in Fig. 3. In literature relative

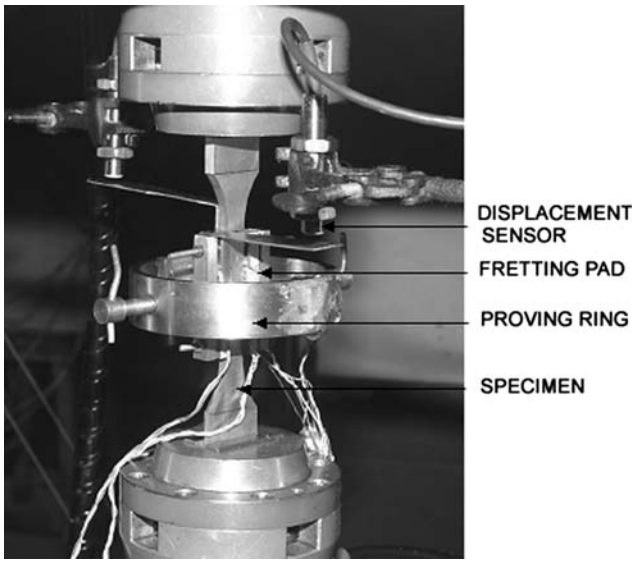

Fig. 3 Photograph of fretting fatigue test setup mounted in a testing machine

slip has been measured by extensometers and/or strain gauges of different configurations (for example, see Refs. [15–17]). The common principle in these procedures is the measurement of relative displacement between two points, one on the fretting pad and other on specimen. Ideally, the two measurement points should be as close as possible to contact surface. However, this condition cannot be satisfied due to practical experimental difficulties. So the measurements give only the apparent or global slip value, which are considerably larger than the actual relative slip at the contact surface. It should be kept in mind that the relative slip values reported in the present study are apparent or global relative slip values.

Fretting fatigue tests were conducted at a stress ratio of 0.1 in pulsating tension in laboratory air (approximately 60–70% relative humidity) at room temperature on a Schenck servo-hydraulic machine at different cyclic stress levels with a cycle frequency of 10 Hz. The contact pressure was maintained at 100 MPa. Fretting pads having three different pad spans (15, 20 and 30 mm) were used. The frictional force and relative slip between the fretting pads and the specimen were recorded throughout the tests by means of a strain amplifier and data acquisition system (HBM–Spider 8–600 Hz and catman Express 4.0 software).

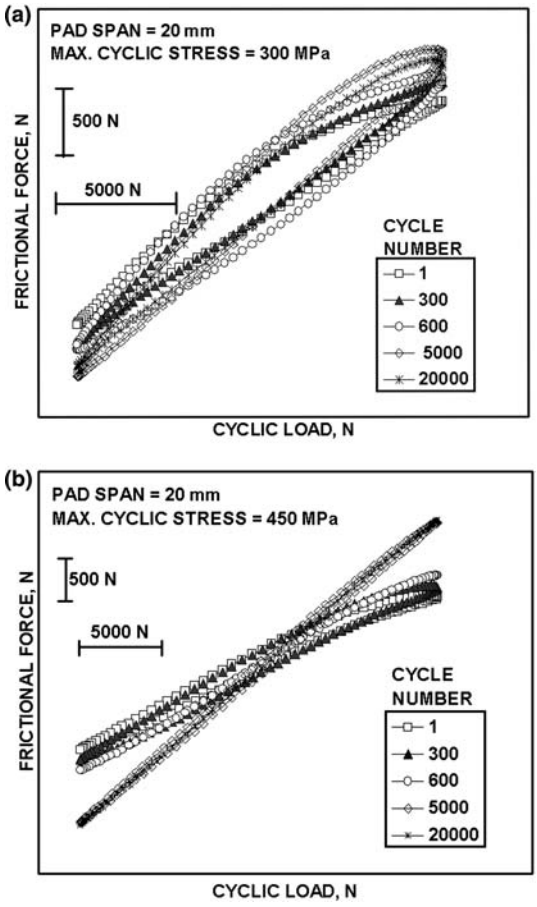

Fig. 4 Variation of frictional force with cyclic load at different no. of cycles. (**a**) Max. stress = 300 MPa, (**b**) Max. stress = 450 MPa

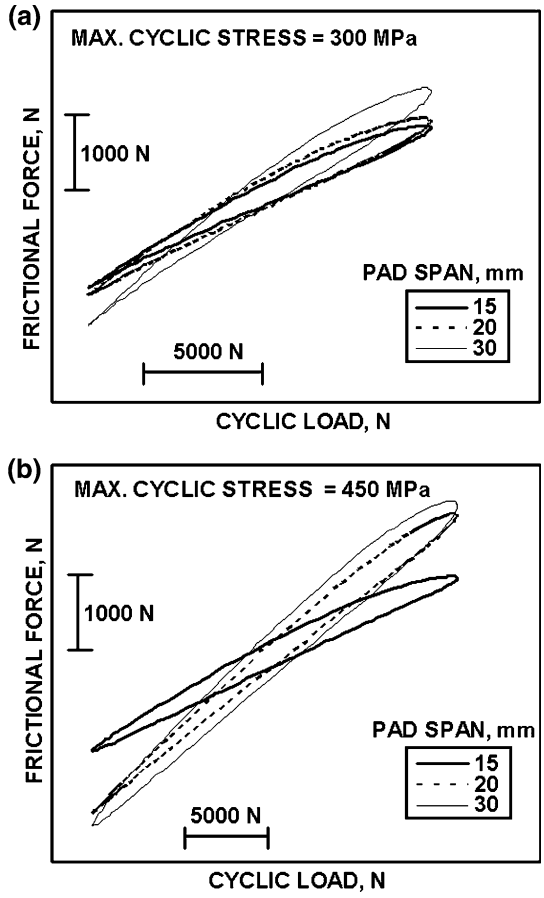

Fig. 5 Variation of frictional force in stabilized condition with cyclic load at different maximum stress levels. (**a**) 300 MPa; (**b**) 450 MPa

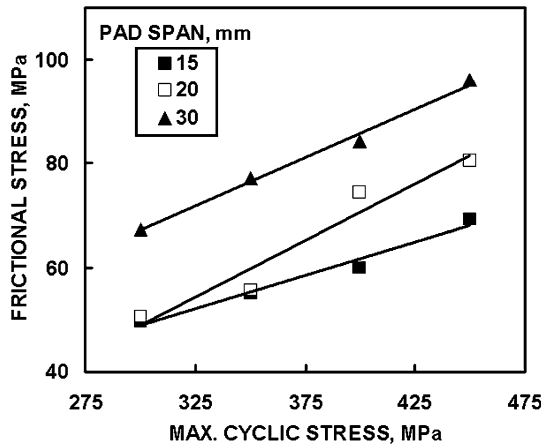

Fig. 6 Variation of stabilized value of frictional stress with maximum cyclic stress

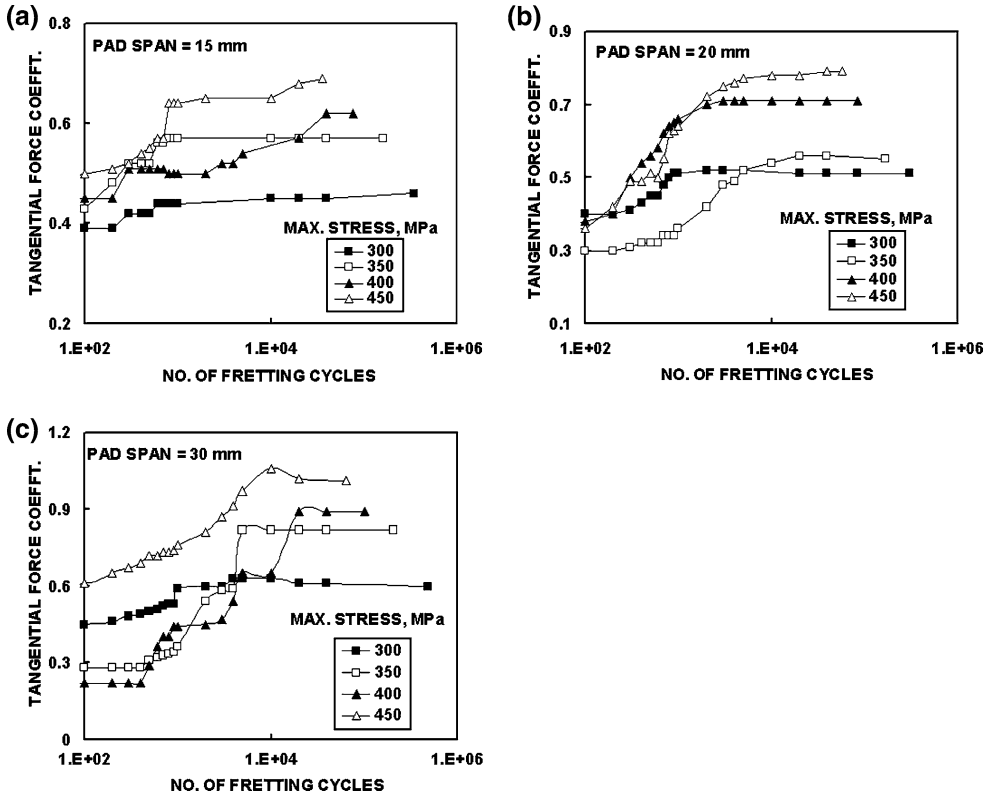

Fig. 7 Variation of tangential force coefficient with no. of fretting cycles for three different pad span values. (**a**) 15 mm, (**b**) 20 mm, (**c**) 30 mm

The fretting scar regions in the tested specimens were observed at low magnifications and photographs were taken using a digital camera. As the test material AISI 304 austenitic stainless steel was metastable at room temperature, it underwent deformation-induced martensitic transformation during testing. The evidence for transformation products (α' and ε martensite) was checked using optical microscopy, transmission electron microscopy and X-ray diffraction (XRD). The content of magnetic phase α'-martensite was measured using a Helmut Fischer ferritescope.

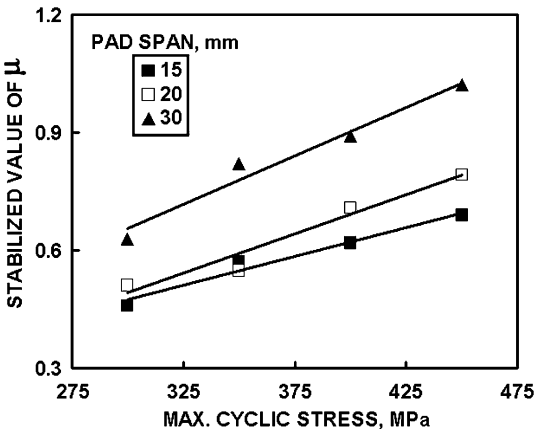

Fig. 8 Variation of stabilized value of tangential force coefficient, μ with max. cyclic stress

Results and discussion

Frictional (tangential) force vs. cyclic load hysteresis-type loops (friction loops) for the material tested with fretting pads having 20 mm pad span at two different cyclic stress levels (300 and 450 MPa) for different number of cycles are shown in Fig. 4. The shape and size of the loop changed with an increase in number of cycles. In the initial stages the loop was little wider and shorter. The loop became narrow and the slope value increased as the number of cycles increased. After reaching about 20,000 cycles the loop size and shape did not change and a stabilized condition was reached. The variation of frictional force in the stable condition (after 20,000 cycles) with cyclic load corresponding to three different pad spans at two different cyclic stress levels (300 and 450 MPa) is shown in Fig. 5. As the pad span increased, the friction force value increased.

The effect of pad span on the stabilized value of frictional stress (=frictional force/contact area) at different cyclic stress levels is shown in Fig. 6. The frictional force is considered to be created by either direct interlocking of surface asperities, or by trapped oxide

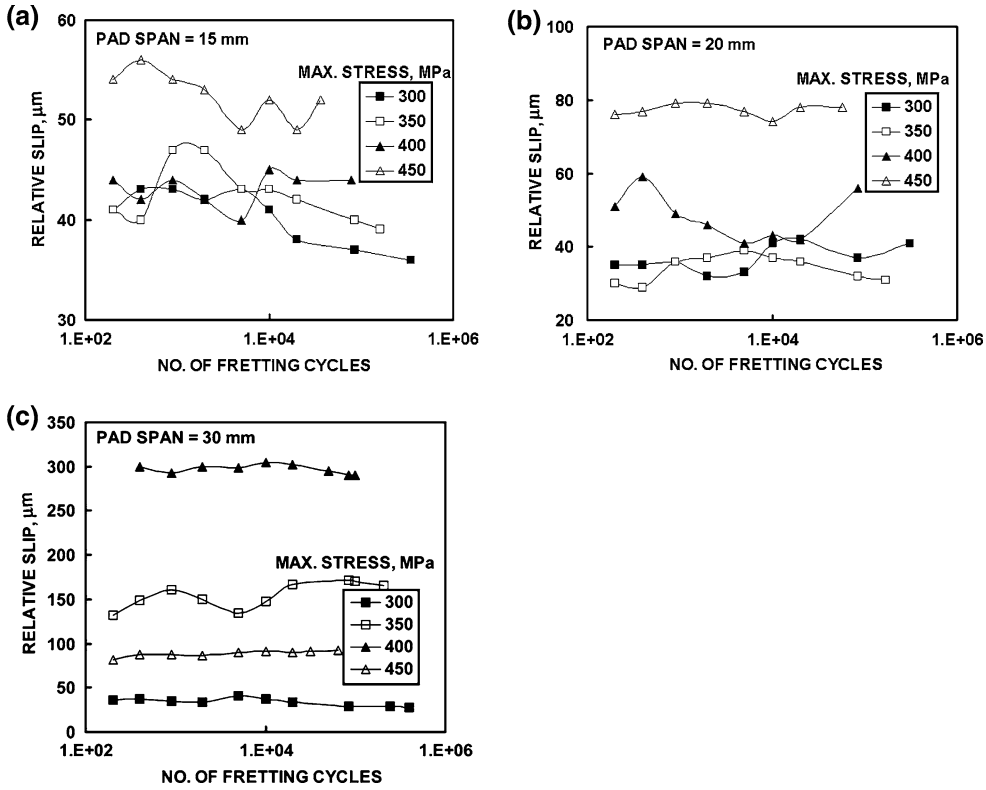

Fig. 9 Variation of relative slip range (at half life) with no. of fretting cycles for three different pad span values. (**a**) 15 mm, (**b**) 20 mm, (**c**) 30 mm

debris in between the surface asperities. At the beginning of the test, friction was created by direct interlocking of surface asperities. At low applied cyclic stress, the contacting surfaces were essentially locked together and there was no significant relative slip. As the applied cyclic stress increased, relative slip was apparent and slight surface fretting damage was apparent as a scar. For a given applied cyclic stress as the pad span increased, the frictional force (stress) increased.

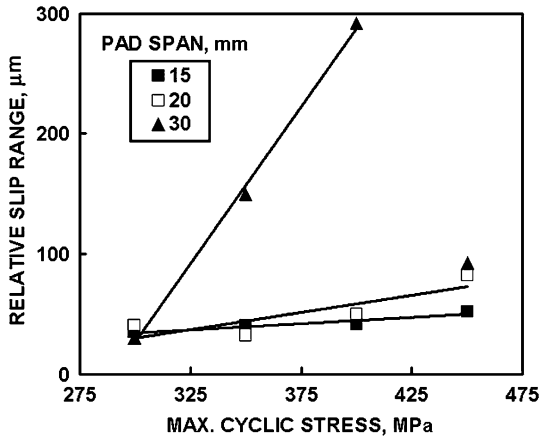

Fig. 10 Variation of relative slip with maximum cyclic stress

The variation of tangential force coefficient (frictional force/contact force), μ with number of cycles at various cyclic stress levels corresponding to three different pad spans is shown in Fig. 7. In all cases there was a rapid increase in the tangential force coefficient value followed by a steady-state condition. Also, the tangential force coefficient increased with the applied cyclic stress. In the initial period there was a gradual build up in the magnitude of frictional forces and there was a reduction in the degree of macro-slip. During the macro-slip conditions, larger contacting asperities were worn out leading to an increase in the area of asperity contact, which promoted micro-slip conditions. After certain number of cycles, under micro-slip conditions, a point was reached where the entire frictional load caused only elastic deformation of contacting asperities [18]. Simultaneously the surfaces were progressively roughened. This roughening was the result of: (1) the welding and tearing of the small metal fragments, which subsequently oxidized; (2) ploughing of asperities on one surface through the other surface; and (3) the pit digging, by abrasion, of the hard oxide particles entrapped in the interface. Mechanical locking of the roughened surfaces could also be a source of friction. The complex interaction of increased surface roughening and increased surface separation might have produced a temporary equilibrium situation where the

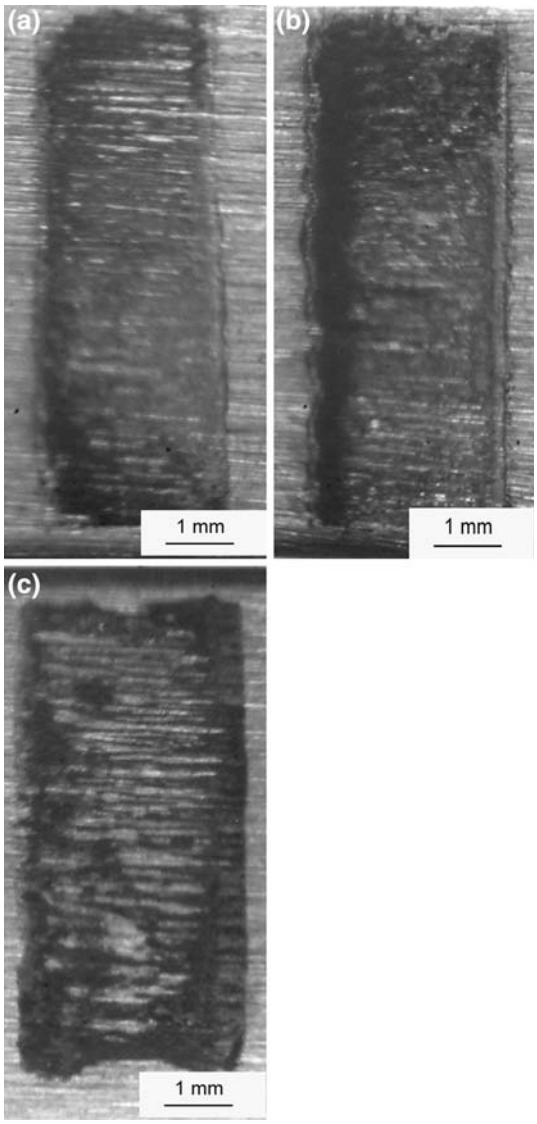

Fig. 11 Appearance of fretting scar in specimens tested at a stress of 350 MPa using pads of different spans. (**a**) 15 mm, (**b**) 20 mm, (**c**) 30 mm

friction remained nearly constant throughout the remainder of the fretting fatigue life time. The influence of pad span on the stabilized value of tangential force coefficient is shown in Fig. 8. The tangential force coefficient increased with an increase in pad span.

The variation of relative slip range with respect to number of cycles at various cyclic stress levels for specimens tested with pads having three different pad spans is shown in Fig. 9. In cases of 15 and 20 mm pad spans the relative slip increased with applied stress level. On the other hand, in case of 30 mm pad span as the applied stress was increased from 300 to 400 MPa, the relative slip range increased. However, at 450 MPa the relative slip range value decreased to a value much

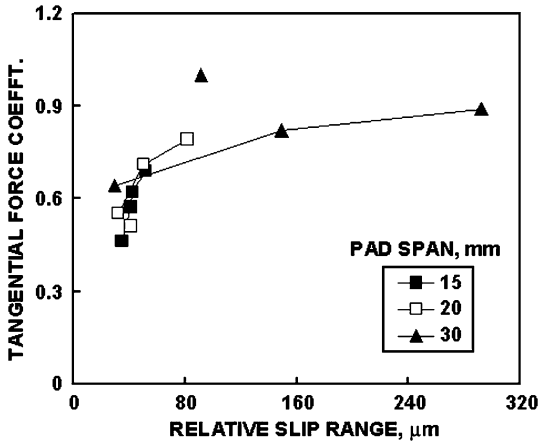

Fig. 12 Variation of stabilized value of μ with half-life relative slip range

lower than that corresponding to 350 MPa. This is an unusual behaviour and the reason for this could not be found out.

The influence of pad span on the relative slip range (half life values) is shown in Fig. 10. As the relative slip range was not constant throughout the test duration, half-life value was considered. There was not much difference between the relative slip range values corresponding to pad span of 15 and 20 mm. However, it may be said that as the pad span increased to 30 mm, the relative slip value increased drastically except that at 300 MPa cyclic stress level. This was reflected in the width of fretting scar. The fretting scar width was more in case of specimens tested with pads having a span of 30 mm (see Fig. 11).

The stabilized value of tangential force coefficient increased with half-life value of relative slip range (see Fig. 12). Though the data point corresponding to 30 mm pad span at 450 MPa is shown in the figure, it was not connected with other data points for 30 mm

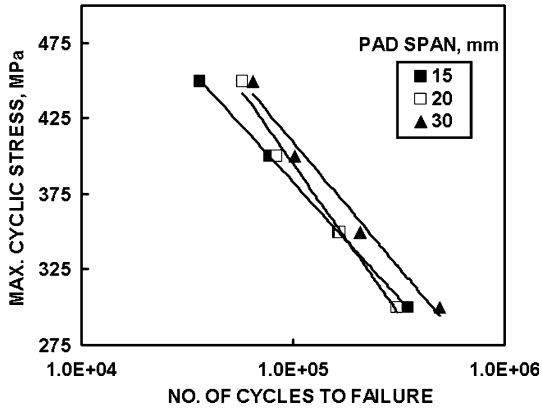

Fig. 13 Effect of pad span on fretting fatigue life

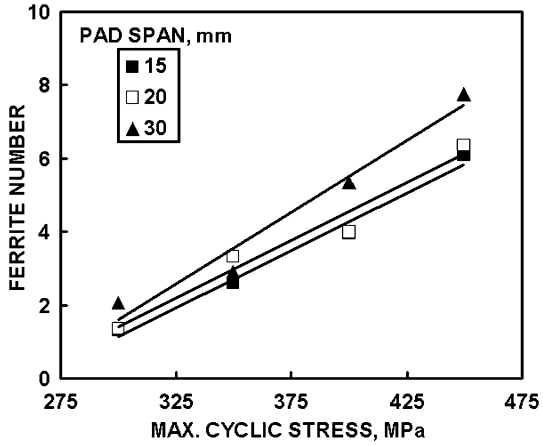

Fig. 14 Effect of pad span on martensite formation

span due to the unusual and unexplained behaviour. The effect of pad span on fretting fatigue life is shown in Fig. 13. The data points corresponding to pad spans of 15 and 20 mm were closely spaced at all stress levels except those at 450 MPa stress level. The relative slip values were almost the same for pad spans of 15 and 20 mm at all stress levels except those at 450 MPa stress level. The relative slip was more for the pad span of 20 mm at 450 MPa compared with that for 15 mm, so the life was superior. The specimens tested with fretting pads having a pad span of 30 mm exhibited superior lives.

There are reports indicating that as pad span increased fretting fatigue life decreased, e.g. Ref. [4, 9]. This was attributed to higher frictional forces generated by longer pad span under micro slip conditions. Jin and Mall [19] have reported that fretting fatigue life of Ti–6Al–4V decreased initially as the relative slip range increased, reached a minimum at a relative slip range of 50–60 μm and then increased with further increase in relative slip range. The increase in fretting fatigue life at larger relative slip range values (>60 μm) was attributed to material removal due to gross slip.

In the present study the frictional stress and tangential force coefficient increased with an increase in pad span. However, for 30 mm pad span the relative slip range was larger compared with 15 or 20 mm pad spans. At the stress levels of 350, 400, 450 MPa very large slip conditions were experienced in case of 30 mm pad span (88–292 μm). It was assumed that due to very large slip small cracks initiated by fretting fatigue mechanism might have been worn away resulting in longer lives. However, to prove this microscopic observations on tested samples are to be carried out.

The evidence for the deformation-induced martensitic transformation was obtained using optical microscopy, X-ray diffraction and transmission electron microscopy. The details are given elsewhere [20]. In all tested specimens the amount of magnetic phase α'-martensite formed in fretting scar region was determined using a ferritescope. As the specimens tested with pads having 30 mm span exhibited longer lives, more martensite formed compared with the specimens tested with pads having 15 or 20 mm pad span (see Fig. 14).

Conclusions

With an increase in pad span, frictional stress, tangential force coefficient and relative slip range increased. Owing to very large relative slip experienced by specimens tested with pads having longer pad span, cracks initiated by fretting might have been worn away resulting in longer lives. More martensite formed in specimens tested with pads having longer pad span due to superior lives.

Acknowledgement This work was supported by the Department of Science and Technology, Government of India under SERC Fast Track Scheme 2001–2002 (project number SR/FTP/ET-183/2001).

References

1. Waterhouse RB (1992) Inter Mater Rev 37:77
2. Dobromirski JM (1992) In: Attia MH, Waterhouse RB (eds) Standardization of fretting fatigue test methods and equipment, ASTM STP 1159. American Society for Testing and Materials, Philadelphia, USA, p 60
3. Nishioka K, Hirakawa K (1969) Bull JSME 12:180
4. Sato K, Fuji H (1984) J Jpn Soc Mech Eng 53:196
5. Vingsboro O, Soderberg S (1988) Wear 126:131
6. Fouvry S, Kapsa P, Vincent L (1996) Wear 200:131
7. Favrow LH, Werner D, Pearson D, Brown KW, Lutian MJ, Annigeri BS, Anton DL (2000) In: Hoeppner DW, Chandrasekaran V, Elliot CB (eds) Fretting fatigue: current technologies and practices, ASTM STP 1367. American Society for Testing and Materials, West Conshohocken, USA, p 391
8. Anton DL, Lutian MJ, Favrow LH, Logan D, Annigeri BS, ibid, p 119
9. Sabelkin V, Martinez SA, Mall S, Sathish S, Blodett MP (2004) Fatigue Fract Eng Mater Struct 28:321
10. Gao HS, Gu HC, Zhou H (1991) Wear 148:15
11. Nix KG, Lindley TC (1988) Wear 125:62
12. Spink JM (1990) Wear 136:281
13. Hills DA, Nowell D (1994) In: Mechanics of fretting fatigue. Kluwer Academic Publishers, Dordreht, The Netherlands, p 165
14. Ramakrishna Naidu NK, Ganesh Sundara Raman S (2005) Int J Fatigue 27:323
15. Wittkowsky BU, Birch PR, Dominguez J, Suresh S (1999) Fatigue Fract Eng Mater Struct 22:307

16. Ochi Y, Kido Y, Akiyama T, Matsumura T (2003) In: Mutoh Y, Kinyon S, Hoeppner DW (eds) Fretting fatigue: advances in basic understanding and applications, ASTM STP 1425. American Society of Testing and Materials, West Conshohocken, PA, USA, p 220
17. Puglia A, Pratesi F, Zonfrillo G (1994) In: Waterhouse RB, Lindley TC (eds) Fretting fatigue, ESIS 18. Mechanical Engineering Publications, London, UK, p 219
18. Rayaprolu DB, Cook R (1992) In: Attia MH, Waterhouse RB (eds) Standardization of fretting fatigue test methods and equipment, ASTM STP 1159. American Society for Testing and Materials, Philadelphia, USA, p 129
19. JIN O, Mall S (2002) Wear 253:585
20. Ganesh Sundara Raman S, Jayaprakash M (2007) Mater Sci Technol 23:45